J Physiol 587.3 (2009) pp 625–640

The Journal of Physiology

De novo expression of Kv6.3 contributes to changes in vascular smooth muscle cell excitability in a hypertensive mice strain

Alejandro Moreno-Domínguez, Pilar Cidad, Eduardo Miguel-Velado, José R. López-López and M. Teresa Pérez-García

Departamento de Bioquímica y Biología Molecular y Fisiología e Instituto de Biología y Genética Molecular (IBGM), Universidad de Valladolid y Consejo Superior de Investigaciones Científicas (CSIC), c/Sanz y Forés s/n, 47003 Valladolid, Spain

Essential hypertension involves a gradual and sustained increase in total peripheral resistance, reflecting an increased vascular tone. This change associates with a depolarization of vascular myocytes, and relies on a change in the expression profile of voltage-dependent ion channels (mainly Ca^{2+} and K^+ channels) that promotes arterial contraction. However, changes in expression and/or modulation of voltage-dependent K^+ channels (Kv channels) are poorly defined, due to their large molecular diversity and their vascular bed-specific expression. Here we endeavor to characterize the molecular and functional expression of Kv channels in vascular smooth muscle cells (VSMCs) and their regulation in essential hypertension, by using VSMCs from resistance (mesenteric) or conduit (aortic) arteries obtained from a hypertensive inbred mice strain, BPH, and the corresponding normotensive strain, BPN. Real-time PCR reveals a differential distribution of Kv channel subunits in the different vascular beds as well as arterial bed-specific changes under hypertension. In mesenteric arteries, the most conspicuous change was the *de novo* expression of Kv6.3 (*Kcng3*) mRNA in hypertensive animals. The functional relevance of this change was studied by using patch-clamp techniques. VSMCs from BPH arteries were more depolarized than BPN ones, and showed significantly larger capacitance values. Moreover, Kv current density in BPH VSMCs is decreased mainly due to the diminished contribution of the Kv2 component. The kinetic and pharmacological profile of Kv2 currents suggests that the expression of Kv6.3 could contribute to the natural development of hypertension.

(Received 20 October 2008; accepted after revision 12 December 2008; first published online 15 December 2008)
Corresponding author M. Teresa Pérez-García: Departamento de Fisiología, Universidad de Valladolid, Edificio IBGM, c/ Sanz y Forés s/n, 47003 Valladolid, Spain. Email: tperez@ibgm.uva.es

Vascular tone plays an important role in the regulation of blood pressure and the distribution of blood flow between and within organs of the body. Vascular tone is determined by the contractile state of vascular smooth muscle cells (VSMCs) within the blood vessel wall, which is regulated by a complex interplay of vasodilator and vasoconstrictor stimuli. Contraction of VSMCs is ultimately dependent on an increase of intracellular calcium concentration ($[Ca^{2+}]_i$). The major pathways for this increase are the influx through voltage-dependent Ca^{2+} channels (VDCC) and non-selective cation channels at the plasma membrane or release from intracellular stores through the internal store release channels. Global $[Ca^{2+}]_i$ is mainly regulated by the open probability of VDCC, which is finely controlled by the membrane potential (E_M). Thus, there is a close coupling between E_M, Ca^{2+} influx, $[Ca^{2+}]_i$ and force maintenance in VSMC, implying that factors that modulate E_M have a direct effect on contraction and vascular resistance.

As VSMCs' resting E_M is dominated by K^+ permeability, these channels play a central role in regulating vascular tone. The molecular characterization of ion channels has improved our knowledge of the physiology of VSMCs, and the scenario has became increasingly precise and also increasingly complex. Functional expression of four different classes of K^+ channels has been identified in VSMCs: voltage-activated (Kv), large-conductance Ca^{2+}-activated (BK_{Ca}), inward rectifiers (K_{IR}, including the ATP-sensitive), and two-pore domain K^+ (K_{2P}) channels (Nelson & Quayle, 1995; Jackson, 2000; Cox, 2002; Cox & Rusch, 2002). To date, the most accepted

A. Moreno-Domínguez and P. Cidad contributed equally to this work.

DOI: 10.1113/jphysiol.2008.165217

model to explain the electrical remodelling of VSMCs in hypertension postulates the existence of a characteristic expression pattern of Ca^{2+} and K^+ channels, more precisely, an increase in the expression of VDCC together with a decrease in the expression of K_V channels and a compensatory over-expression of the BK_{Ca} channels. This expression remodelling would favour depolarization, Ca^{2+} influx and increased vascular tone (Cox & Rusch, 2002).

Under physiological conditions, Kv currents contribute to determine resting E_M of VSMCs and consequently vascular tone, providing a tonic negative feedback system in response to small depolarizations induced by increases in blood pressure (Cheong *et al.* 2001*a*; Chen *et al.* 2006). Electrophysiological studies show a decreased functional expression of Kv channels in hypertensive animals, which would contribute to VSMC depolarization (Nelson & Quayle, 1995; Jackson, 2000; Cox & Rusch, 2002). However, the molecular diversity of these channels (Coetzee *et al.* 1999), together with the variations in their expression in the different vascular beds, has complicated the determination of their precise functional role and their changes in hypertensive models. There are indications that Kvα subunits are differentially expressed depending on the size of blood vessel and on the vascular bed (Fountain *et al.* 2004), and in some studies a correlation between the mRNA expression levels of some Kv subunits and their functional contribution to VSMC excitability has been explored (Cheong *et al.* 2001*b*; Albarwani *et al.* 2003; Plane *et al.* 2005; Chen *et al.* 2006; Yeung *et al.* 2007; Mackie *et al.* 2008). The study of the changes in expression of K_V channels (and their functional contribution) in hypertensive models has not been addressed in such a systematic way. Notwithstanding, this information is relevant to understand the ionic mechanisms that alter vascular reactivity in this pathology and to develop new vasoactive drugs, which may rely on targeting disease-specific changes in ion channel expression as antihypertensive therapy.

In the present study we have explored the expression levels of Kv channel subunits in conduit *versus* resistance vessels and in normotensive *versus* hypertensive animals. The experimental models that better reproduce essential hypertension in humans are those obtained by phenotypic selection from natural variants, maintained with inbreeding. Using this approach, endogamous strains of hypertensive rats (SHR, in which most of the hypertension studies in animal models have been carried out) and hypertensive and hypotensive mice have been developed (Schlager & Sides, 1997). Phenotypic selection of crossbreeding between eight different mice strains allowed the identification of hypertensive (BPH), hypotensive (BPL) and normotensive (BPN) lines sharing a comparable genetic background. A differential display of genes modified in these two models of hypertension (SHR rats and BPH mice) suggests the existence of fundamental transcriptional mechanisms in common between them, spanning a diverse set of biological processes, which reinforces the multifactorial and complex nature of hypertension (Friese *et al.* 2005).

Using VSMCs from resistance arteries (i.e. 2nd–3rd branches of mesenteric arteries) from BPN and BPH mice, we have determined the expression profile of Kv channels and studied their contribution to VSMCs' currents and excitability. The results of this channel-wide characterization show that the most remarkable change observed in the mRNA expression profile of mesenteric VSMCs from BPH mice is the *de novo* expression of Kv6.3, and the functional studies indicate that this change could explain the differences in Kv current amplitude and kinetics observed in these cells, suggesting that the remodelling of Kv2 current could be an important determinant of the hypertensive phenotype in resistance arteries.

Methods

Ethical approval

BPN and BPH mice (Jackson Laboratories) were maintained with inbred crossing in the animal facility of the School of Medicine of Valladolid. Animals were housed under temperature-controlled conditions (21°C) and had free access to water and food. All animal protocols were approved by the Institutional Care and Use Committee of the University of Valladolid, and are in accordance with the European Community guiding principles in the care and use of animals.

Blood pressure measurement

Blood pressure was measured in awake mice with a tail cuff pressure meter (LSI Letica Scientific Instruments, Barcelona, Spain). We monitored systolic (SP) and diastolic pressure (DP) and calculated medium pressure (MP) as $MP = DP + 0.33(SP - DP)$. Average pressure values (in mmHg) were for SP 135.2 ± 1.9 in BPN *versus* 152.6 ± 3.1 in BPH ($P < 0.001$) and for DP 90.4 ± 3.5 in BPN *versus* 106.0 ± 3.4 in BPH ($P < 0.001$ in both cases).

VSMC isolation

Mice were killed by decapitation after isofluorane anaesthesia (5% at 2.5 l O_2 min^{-1}). VSMCs from mesenteric arteries were obtained after carefully dissection and cleaning of connective and endothelial tissues. Afterwards, VSMCs were either frozen at −80°C to further extract RNA and proteins or used directly to obtain fresh dispersed VSMCs. Small pieces of endothelium-free mesenteric artery were placed in smooth muscle dissociation solution (SMDS) Ca^{2+} free solution

containing 0.6 mg ml^{-1} papain (Worthington), 1 mg ml^{-1} BSA (Sigma) and 1 mg ml^{-1} dithiothreitol (DTT; Sigma) and incubated at 37°C for 15 min in a shaking water bath. After two washings in SMDS–10 μM Ca^{2+} a second 12 min incubation was performed with SMDS 10 μM Ca^{2+} in a 0.56 mg ml^{-1} collagenase F, 0.24 mg ml^{-1} collagenase H (Sigma) and 1 mg ml^{-1} BSA solution. Single cells were obtained by gentle trituration with a wide-bore glass pipette, stored at 4°C and used within the same day. Ionic composition of SMDS was (in mM): NaCl 145; KCl 4.2; KH_2PO_4 0.6; $MgCl_2$ 1.2; Hepes 10; glucose 11, pH adjusted to 7.4 with NaOH.

RNA isolation, RT and real time PCR

Total RNA from arteries was isolated with MELT™ Total RNA Isolation System Kit (Ambion, Inc., Austin, TX, USA) following the manufacturer's instructions. Five to six second- and third-order mesenteric arteries and the thoracic aorta of five mice were employed for each determination. The quality of the RNA was assayed by OD measurement at 260 and 280 nm and by electrophoresis on agarose gels. After DNAse I (Ambion) treatment, 500–750 ng of RNA was reverse transcribed with MuLvRT (5000 μ ml^{-1}) in the presence of 20 u μl^{-1} of RNAse inhibitor, 50 μM Random Hexamers, 10× PCR buffer, 25 mM $MgCl_2$ and 10 mM mixed dNTPs at 42°C for 60 min, to get cDNA (RT+). All reagents were from Applied Biosystems (Foster City, CA, USA). From the same samples, 200–350 ng of total RNA was used as genomic control in reverse transciptase reaction in the absence of MuLv and RNase Inhibitor at 42°C for 60 min (RT–). A small fraction of these cDNAs was used for real-time amplifications of selected control genes (*GAPDH* and *Gus*) in a Rotor-Gene RG3000 thermocycler (Corbett Life Science, Sydney, NSW, Australia). Primer sets and TaqMan probes for these genes were:

mGAPDH: 5′-TGTGTCCGTCGTGGATCTG-3′, 5′-GATGCCTGCTTCACCACCTT-3′ and 5′-FAM-TGGAGAAACCTGCCAAGTATGATGACATCA-BHQ2–3′;

mGus: 5′-CAATGGTACCGGCAGCC-3′, 5′-AAGCTAGAAGGGACAGGCATGT-3′ and 5′-FAM-TACGGGAGTCGGGCCCAGTCTTG-BHQ2–3′.

Amplifications were performed in 20 μl final volume, using 10 μl of Absolute QPCR mix (ABgene, Epsom, UK), 1 μl of each primer, 1 μl of the probe and 1 μl of cDNA. Cycling conditions were 15 min at 95°C, and 40 cycles of 95°C for 15 s, followed by 60°C for 1 min. These amplifications were used to compare the different samples, and also to check the efficiency of the DNAse treatment by comparing expression levels of the gene between RT+ and RT– samples.

Real-time PCR was carried out with TaqMan Low Density Arrays (Applied Biosystems). These cards were processed by the Genomic Service of the CNIC (Madrid, Spain), with the ABI Prism 7900HT Sequence detection system (Applied Biosystems). Data were acquire with SDS 2.1 software (Applied Biosystems) and analysed using the threshold cycle (C_t) relative quantification method ($\Delta\Delta C_t$) (Livak & Schmittgen, 2001). Expression data of genes were normalized by the internal control, 18S ribosomal RNA. The relative abundance of the genes was calculated from $2^{(-\Delta C_t)}$, where $\Delta C_t = C_{t,\mathrm{Channel}} - C_{t,18S}$. Differences between hypertensive and normotensive VSMCs were calculated from $2^{(-\Delta\Delta C_t)}$, where $\Delta\Delta C_t = \Delta C_{t(\mathrm{BPH})} - \Delta C_{t(\mathrm{BPN})}$. For comparisons, the $\Delta C_{t(\mathrm{BPN})}$ was designated as the calibrator, and the data in BPH samples are presented as the fold change in gene expression. In order to do statistical comparisons, ΔC_t values obtained in each sample ($C_{t,\mathrm{Channel}} - C_{t,18S}$), were subtracted from the mean ΔC_t of the calibrator to provide the S.E.M. Each data point was obtained from duplicate determinations from at least five different assays. In the cases in which expression of a gene was not detected in one of the conditions, a C_t value of 40 was assigned in order to do the comparisons.

Immunoblots

For total protein isolation, 20–25 mesenteric arteries obtained from five to six animals were placed in lysis buffer (50 mM Tris pH 8, 150 mM NaCl, 1% NP-40, 0.5% sodium deoxicolate, 0.1% SDS) with protease inhibitors (1 mM benzamidine, 1 mM phenylmethylsulphonyl fluoride, 1 mM DTT, 5 μg ml^{-1} aprotinin, 5 μg ml^{-1} leupeptin, and 5 μg ml^{-1} pepstatin A) and homogenized in the Precellys 24 homogenizator (Bertin Technologies) using ceramic beads (CK14). Samples of 25 μg of tissue proteins with XT Reducing Agent (BIO-RAD) and XT Sample Buffer (Bio-Rad) were heated for 5 min at 95°C. Proteins were separated by SDS-PAGE (Criterion™ Precast Gel 10% Bis-Tris, Bio-Rad) and transferred onto polyvinylidene difluoride (PVDF) membrane. After blockade of the membranes with 5% non-fat dry milk in TTBS (TBS with 0.1% Tween 20), membranes were incubated with either mouse polyclonal anti-Kv6.3 antibody (KCNG3-A01, Abnova Corp., Taipei City, Taiwan) or mouse monoclonal anti-β-actin (mAbcam 8226) in blocking solution at a final concentration of 1 : 1000 for 1 h. Membranes were next incubated with horseradish peroxidase-conjugated donkey anti-mouse IgG (Santa Cruz Biotechnology, Inc., Santa Cruz, CA, USA) at a final concentration of 1 : 10000 for 1 h. Protein signals were detected in the VersaDocTM 4000 Image System (Bio-Rad) with SuperSignal® West Femto Maximum Sensitivity Substrate for Kv6.3 and SuperSignal® West Pico Chemiluminescent Substrate for β-actin (Thermo Fisher Scientific Inc., Waltham, MA,

USA). Mouse brain proteins isolated with Trizol reagent (Invitrogen) were used as control.

Histology and immunohistochemistry

Complete mesenteric arteries (with endothelial and connective tissue) were fixed with 4% paraformaldehyde. Arteries were then cleared and embedded in paraffin. Paraffin sections (6 μm) were dewaxed, rehydrated, and stained with haematoxilin–eosin following standard procedures. Measures were done with NIS-Elements software (Nikon) and each value was obtained from triplicate determinations of a second-order mesenteric artery from at least eight mice in each condition.

HEK293 cell maintenance and transfections

HEK293 cells were maintained in Dulbecoo's modified Eagle's medium (DMEM) supplemented with 10% fetal calf serum (Gibco), 100 U ml^{-1} penicillin, 100 g ml^{-1} streptomycin and 2 mM L-glutamine. Cells numbering 2–4 $\times$ 10^5 were grown as a monolayer in 6 mm coverslips placed in the bottom of a 35 mm Petri dish the day prior to transfection. Transient transfections were performed using Lipofectamine 2000 (Invitrogen), with 0.2 μg of plasmid DNA encoding Kv2.1 alone or in combination with 1.2 μg of plasmid DNA encoding Kv6.3 subunit (molar ratio Kv2.1:Kv6.3 1 : 6). In all cases, 0.2 μg of plasmid DNA encoding the green fluorescent protein (GFP) was included to permit transfection efficiency estimates (20–60%) and to identify cells for voltage-clamp analysis. The plasmids pEGFP-N1-Kv2.1 and pEGFP-N1-Kv6.3 (KCNG3) were provided by Dr D. J. Snyders (University of Antwerp, Belgium).

Electrophysiological methods

Ionic currents were recorded at room temperature (20–25°C, RT) using the whole-cell configuration of the patch-clamp technique. The coverslips with the attached HEK cells were placed at the bottom of a small recording chamber (0.2 ml) on the stage of an inverted microscope and perfused by gravity with the bath solution, while freshly isolated VSMCs were placed directly on the recording chamber and left to settle for a few minutes before starting superfusion with the external solution. Patch pipettes were made from borosilicate glass (2.0 mm O.D., WPI) and double pulled (Narishige PP-83) to resistances ranging from 2 to 5 MΩ for HEK cells and from 7 to 10 MΩ for VSMCs when filled with the internal solution, containing (mM): 125 KCl, 4 $MgCl_2$, 10 Hepes, 10 EGTA, 5 MgATP, pH 7.2 with KOH. The composition of the bath solution was (mM): 141 NaCl, 4.7 KCl, 1.2 $MgCl_2$, 1.8 $CaCl_2$, 10 glucose and 10 Hepes, pH 7.4 with NaOH. Whole-cell currents were recorded using an Axopatch 200 patch-clamp amplifier, filtered at 2 kHz (−3 dB, 4-pole Bessel filter), and sampled at 10 kHz. When leak subtraction was performed, an online *P*/4 protocol was used. Recordings were digitized with a Digidata 1200 A/D interface, driven by Clampex 8 software (Axon Instruments) in a Pentium clone computer.

Current–voltage relationships were obtained from a holding potential of −80 mV in 10 mV depolarizing steps from −60 to +80 mV. Deactivation was studied in symmetrical potassium solutions and tail currents were elicited upon repolarization to −80 mV from 500 ms depolarizing pulses (from −60 to +80 mV) and fitted to a double exponential function.

Kv toxin blockers were acquired from Alomone Laboratories (Jerusalem, Israel), guangxitoxin-1E (GxTx) was a gift from James Herrington (Merck) and correolide was a gift from María García (Merck).

Membrane potential measurements were performed at RT using the perforated-patch technique and recordings were obtained with an Axopatch 4A patch-clamp amplifier. Pipette tips were briefly dipped into a solution containing (in mM): 40 KCl, 95 potassium glutamate, 8 $CaCl_2$, 10 Hepes, pH 7.2, and backfilled with the same solution containing amphotericin B (300 μg ml^{-1}). After obtaining a high-resistance seal, electrical access to cell cytoplasm was assessed by monitoring the increase in cell capacitance. At this point, the amplifier was switched to current-clamp mode and membrane potential was continuously recorded. The high Ca^{2+} content of the pipette solution ensures the correct performance of the perforate-patch technique, as accidental rupture of the patch (changing to whole-cell configuration) leads to a sudden Ca^{2+} load and cell death.

For the functional blockade of the currents with Kv channel antibodies, ionic currents were recorded by 500 ms voltage steps to +40 mV from a holding potential of −80 mV applied every 10 s. Electrodes were dipped in an antibody-free pipette solution and then back-filled with the pipette solution containing the antibody of interest (0.2 μg ml^{-1}). In order to eliminate artefacts due to changes in the access resistance, a 10 ms prepulse to −100 mV was applied, without whole-cell capacitance and access resistance compensation, 100 ms prior to the step to +40 mV. The current response to this prepulse was used to calculate the capacitance (C_m), the access resistance (R_a) and the membrane resistance (R_m) applying the membrane test algorithms described elsewhere (pCLAMP, Axon Instruments). Cells without stable values of R_a were discarded for analysis. The antibodies used were anti-Kv6.3 (Abnova Corp., see above) and anti-Kv3.1 (Alomone Laboratories).

Electrophysiological data analyses were performed with the Clampfit subroutine of the pCLAMP software (Axon Instruments) and with Origin 7.5 software (OriginLab

Corp., Northampton, MA, USA). Pooled data are expressed as means ± standard error of the mean (S.E.M.). Statistical comparisons between groups of data were carried out with Student's two-tailed *t* test for paired or unpaired data, and values of $P < 0.05$ were considered statistically significant.

Results

Kv channels' mRNA relative expression in resistance and conduit arteries and their changes in the hypertensive model

We first studied the expression pattern of the genes encoding Kv channels, Ca^{2+}-dependent K^+ channels (K_{Ca}) and their accessory subunits in mesenteric and aortic vessels. A total of 39 channel genes were studied, together with several control genes such as calponin as a control of VSMCs, endothelial nitric oxide synthase (eNOS) as a control of endothelial cells and RP18S as endogenous control of the qPCR. Channel genes that were not detected in any of the two vascular beds include Kv3.1, Kv9.1, Kv9.2, Kv10.1, Kv11.3, BKβ2, MinK, MiRP1, KChIP1 and KChIP2 subunits. In addition, mesenteric arteries from BPN animals did not express mRNA for Kv1.4, Kv6.3 and KChIP4 channels, whereas in aortic VSMCs we did not detect MiRP2 mRNA. Figure 1*A* and *B* shows the relative abundance of the channel genes expressed in both preparations (26 in mesenteric and 28 in aortic VSMCs from normotensive animals). The expression levels of the

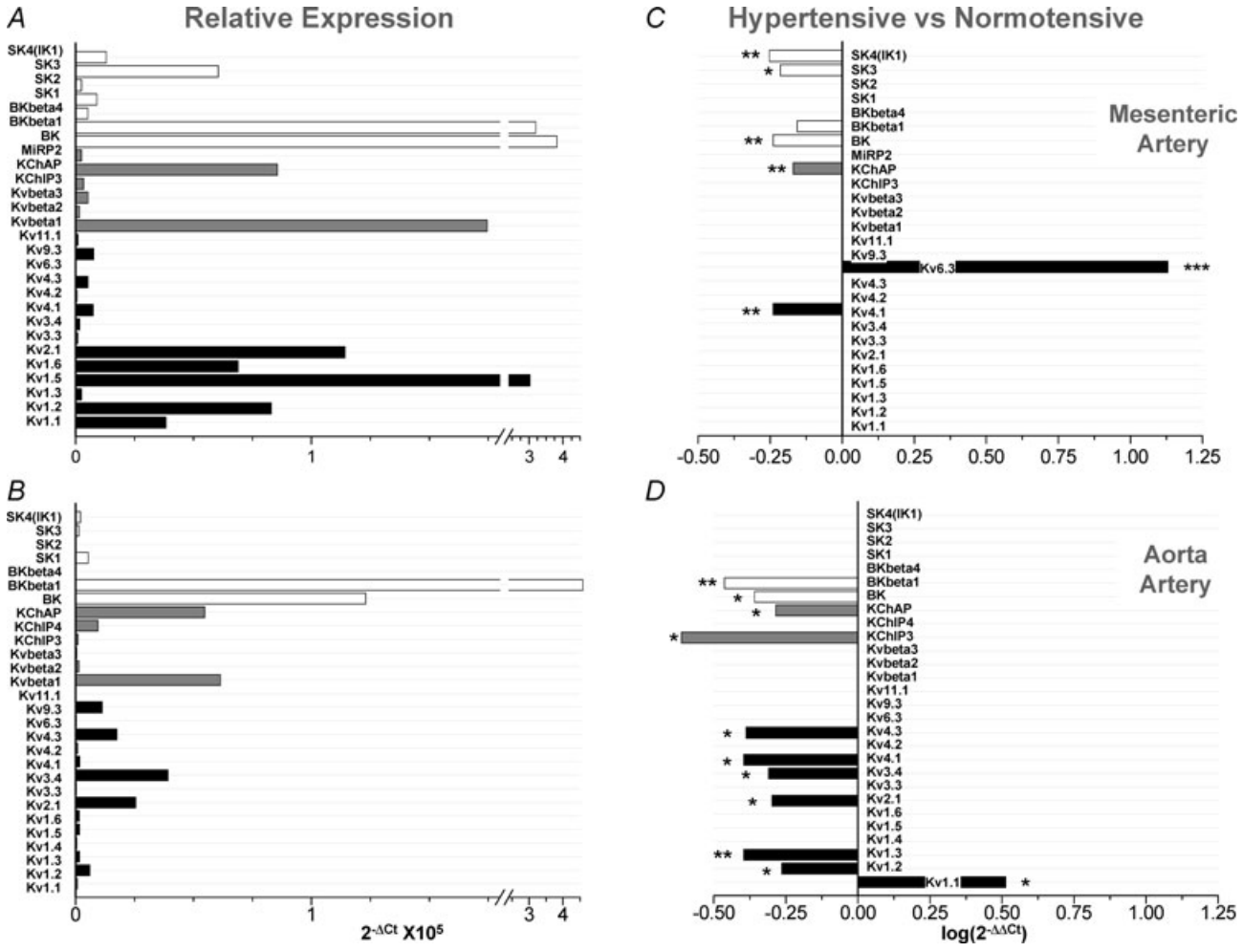

Figure 1. Relative abundance of Kv and K_{Ca} channels in mesenteric (*A*) and aortic VSMCs (*B*)
Expression levels are normalized with respect to RP18s. Relative abundance was expressed as $2^{(-\Delta C_t)}$, where $\Delta C_t = C_{t,channel} - C_{t,18s}$. The plots also show differences in K^+ channels expression in BPH arteries (using BPN expression levels as calibrator) in mesenteric (*C*) and aortic beds (*D*). The changes were calculated as $2^{(-\Delta\Delta C_t)}$, where $\Delta\Delta C_t = \Delta C_{t(BPH)} - \Delta C_{t(BPN)}$, and represented in log scale, so that negative values mean decreased expression and positive values increased expression. Each bar is the mean of 10 determinations obtained in 5 assays by duplicate. All through the figures, $^*P < 0.05$, $^{**}P < 0.01$ and $^{***}P < 0.001$.

mRNA of Kv pore forming subunits, particularly the genes of the Kv1 and Kv2 subfamily, show a increasing pattern (aorta < mesenteric) that correlates with the contribution of these vascular beds to myogenic tone (Plane *et al.* 2005; Cole *et al.* 2005).

Hypertension was associated with vascular bed-dependent changes in the expression of these channel genes (Fig. 1*C* and *D*). In VSMCs from BPH aortas, there was an increased expression of the Kv1.1 gene with a decreased expression of several Kv channel genes from the Kv1–Kv4 subfamilies and also some Kv channel accessory subunits (KChIP3 and KChAP). However, in BPH mesenteric VSMCs, we found changes in the expression of only three Kv genes: KChAP and Kv4.1 decreased their expression and most remarkably Kv6.3 (*Kcng3*) expressed *de novo*, as it was not detected in any of the BPN samples and was present in all the BPH ones. In addition to these changes, we also observed modifications in the expression levels of some members of the K_{Ca} channels, the most conspicuous being the decrease in the expression of mRNA encoding BK_{Ca} channel α and $\beta 1$ subunits, which are the genes with the highest expression level in both aortic and mesenteric VSMCs.

Functional characterization of voltage-dependent outward K^+ currents in mesenteric VSMCs

Following the Kv and K_{Ca} mRNA expression profile in BPN and BPH VSMCs, we explored their functional contribution to the K^+ currents in these cells. This characterization was focused on the study of mesenteric VSMCs, as they are expected to have a higher contribution to vascular resistance than conduit arteries such as aorta.

Outward K^+ currents were studied with the whole-cell patch clamp technique in freshly dissociated VSMCs. Figure 2*A* shows representative traces obtained in one BPN and one BPH cell. Total outward K^+ current density was significantly larger at all voltages in BPN cells (Fig. 2*B*). This fact is partly due to the larger size of BPH cells as compared to BPN ones, as indicated by the capacitance values obtained in both preparations (Fig. 2*B* bars). VSMC hypertrophy in BPH animals is also evident when sections from BPN and BPH arteries are compared (Fig. 2*C*). BPH arteries and media areas were significantly larger, although the number of cells in the media are not different from BPN arteries (Table 1). Since the typical vascular change associated with hypertension is a 'eutrophic' remodelling

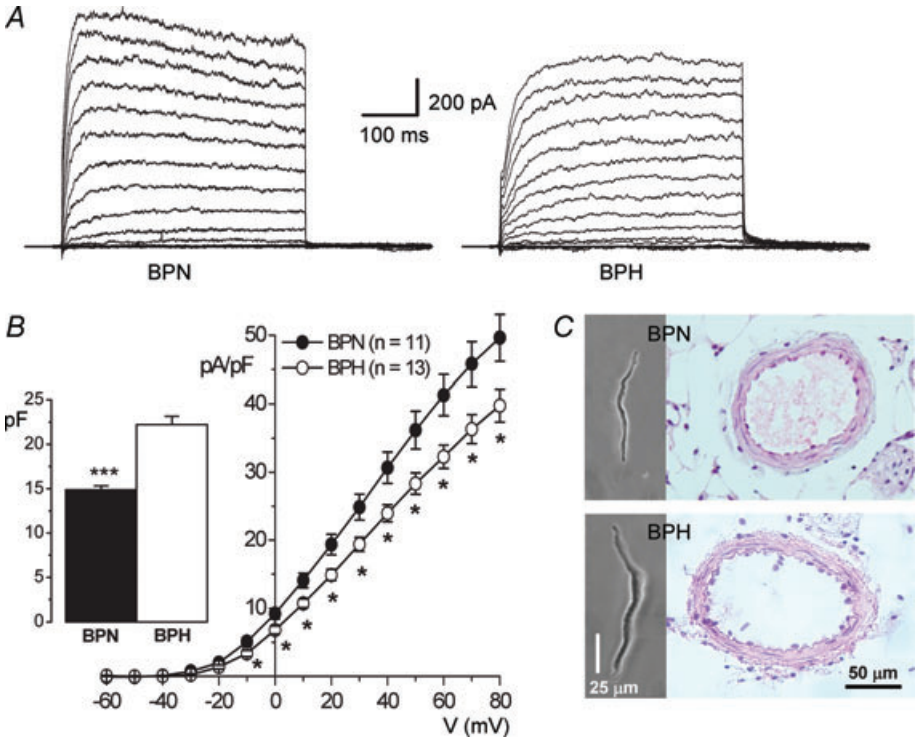

Figure 2. Electrical and morphometrical properties of BPN and BPH mesenteric VSMCs
A, representative total outward K^+ currents obtained in 10 mV depolarizing steps from −60 to +80 mV in one BPN and one BPH mesenteric VSMC. Holding potential was −80 mV and cell capacitance values were 21.0 pF (BPH) and 15.5 pF (BPN). After each step the E_M was held at −50 mV for 200 ms. *B*, BPN (●) and BPH (○) current-density voltage relationships (mean ± S.E.M.) obtained from 12 different cells in each group. The inset shows the mean (± S.E.M.) cell capacitances obtained in both groups; $n = 34$. *C*, representative photomicrographs of BPN and BPH VSMCs dissociated from mesenteric arteries and histological sections of paraffin blocs stained with haematoxylin–eosin.

Table 1. Morphometric parameters obtained from parafine-embedded 2nd order mesenteric arteries

	BPN ($n = 22$)	BPH ($n = 22$)
Weight of the animal (g)	31.5 ± 0.6	28.4 ± 0.5***
Vessel Area (μm^2)	11006.5 ± 628.8	13270.3 ± 481.7**
Luminal Area (μm^2)	6871.3 ± 435.8	8813.5 ± 403.2**
Media area (μm^2)	4021.6 ± 204.4	4604.6 ± 176.4*
Number of cell nuclei in the medium	20.08 ± 0.9	20.8 ± 0.8

(Mulvany, 2002), VSMC hypertrophy observed in BPH animals could reflect either an initial stage in the development of hypertensive status or a response of medium size vessels to distal changes in arterial pressure.

Pharmacological dissection of K^+ currents

We have explored the contribution of the K_{Ca} currents to the total outward K^+ current in whole cell recordings. BK_{Ca} currents were defined as the fraction of the outward current sensitive to paxilline at 500 nM (Li & Cheung, 1999). Figure 3*A* shows representative *I–V* curves, and sample recordings at two different potentials, obtained in VSMCs from BPN and BPH mesenteric arteries before and after paxilline application. Paxilline decreased current amplitude at positive potentials, and this effect was more evident in BPN than in BPH VSMCs. BK_{Ca} represented $19.0 \pm 2.2\%$ of the current density at +80 mV in BPN and $12.74 \pm 1.9\%$ in BPH cells (open circles in Fig. 3*B*). Under these recording conditions (i.e. dialysed VSMCs with a pipette solution containing 10 mM EGTA) the interaction of depolarization and intracellular Ca^{2+} is minimized. For this reason we also explored the contribution of BK_{Ca} currents in perforated-patch recordings, where a physiological $[Ca^{2+}]_i$ is maintained. Figure 3*C* shows the normalized contribution of BK_{Ca} currents to the total outward currents at several voltages in the two experimental conditions (whole-cell and perforated patch) and in the two preparations (BPN

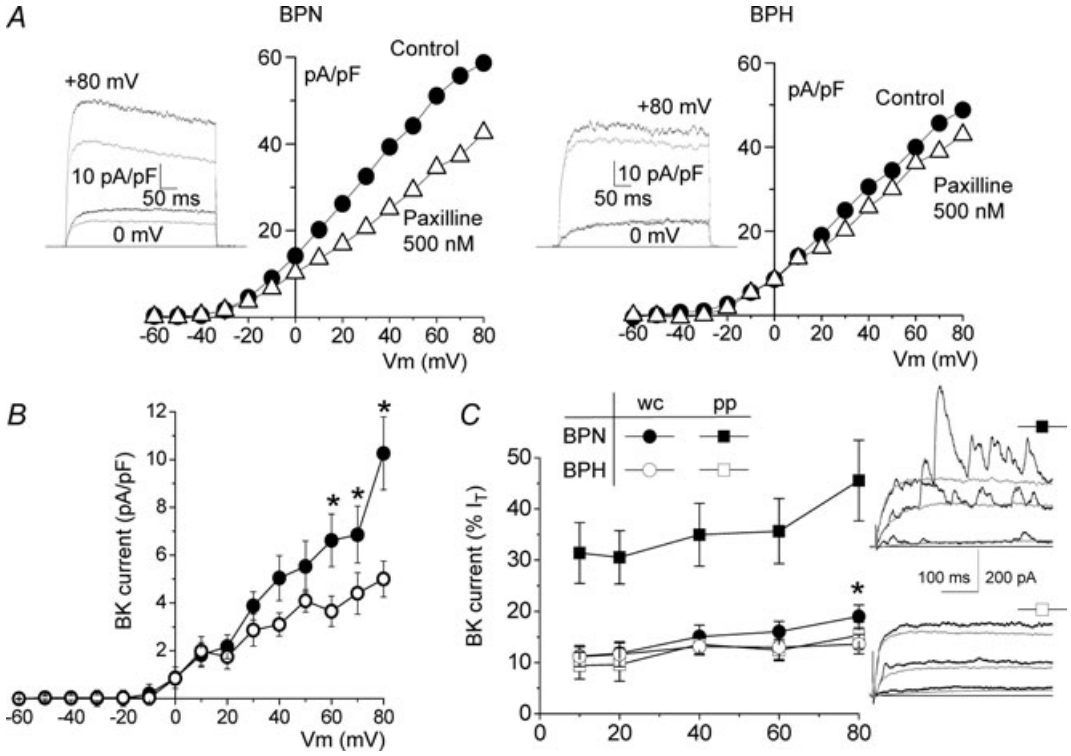

Figure 3. Characterization of BK_{Ca} currents
A, representative current–voltage relationships obtained under control conditions and in the presence of 500 nM paxilline in BPN and BPH cells in whole-cell experiments. Current traces upon depolarization at +80 mV and 0 mV in both conditions are also shown on the left. Grey traces correspond to records in the presence of paxilline. *B*, average paxilline-sensitive *I–V* curves obtained in BPN (●) and BPH cells (○); $n = 16$, whole-cell recordings. *C*, contribution of BK_{Ca} currents in BPN (filled symbols) and BPH cells (open symbols), expressed as a percentage of the total outward current. BK_{Ca} currents were calculated as the difference in the current amplitude at the indicated voltages between control and paxilline traces, both in whole-cell (circles) and in perforated-patch (squares). Data are means ± S.E.M. of 7–15 determinations in each group. *$P < 0.05$ compared to BPH whole-cell data. Representative traces from one BPN and one BPH cell obtained in perforated-patch recordings upon depolarization to +60 mV before and during paxilline application are also shown.

and BPH VSMCs). While in BPN cells there is a significant increase in the proportion of BK_{Ca} current when measured under physiological $[Ca^{2+}]_i$, we found no differences between whole-cell and perforated-patch recordings in BPH cells. These results suggest that both the functional expression of BK_{Ca} channels and their Ca^{2+} sensitivity are reduced in BPH mesenteric VSMCs. The representative traces shown on the right evidence that under perforated-patch conditions spontaneous BK_{Ca} currents events are more frequently observed in BPN cells and have larger amplitudes. Although the mRNA expression profile of mesenteric VSMCs indicates the presence of other members of the K_{Ca} family of channels such as the intermediate (IK1) and small conductance (SK) K_{Ca} channels, apamine (500 nM) had no effect on the outward K^+ currents (data not shown). In fact, the small levels of expression of these other K_{Ca} channels genes could reflect some endothelial contamination, as SK and IK1 expression has been reported in endothelial cells and not in VSMCs (Kohler *et al.* 2003; Jackson, 2005).

Pharmacological characterization of Kv currents

After blockade of BK_{Ca} currents with paxilline, we characterized pharmacologically Kv currents in both preparations. As for BK_{Ca}, Kv current density was significantly larger at all voltages in BPN cells (Fig. 4*A*). The Kv channel gene expression profile in mesenteric arteries (Fig. 1), together with previous data in the literature (Albarwani *et al.* 2003; Fountain *et al.* 2004; Plane *et al.* 2005; Amberg & Santana, 2006) point towards a predominant contribution of Kv1 and Kv2 channels to Kv currents in resistance arteries. A preliminary pharmacological screening directed to determine the proportion of the outward Kv current attributable to the members of the Kv1–Kv4 subfamilies confirmed this extent. Correolide was used to selectively block Kv1 currents (Hanner *et al.* 1999), and differential TEA sensitivity after correolide application allowed the identification of Kv2 and Kv3 currents (Miguel-Velado *et al.* 2005). The TEA and correolide-insensitive currents could be attributed to Kv4 currents (Coetzee *et al.* 1999).

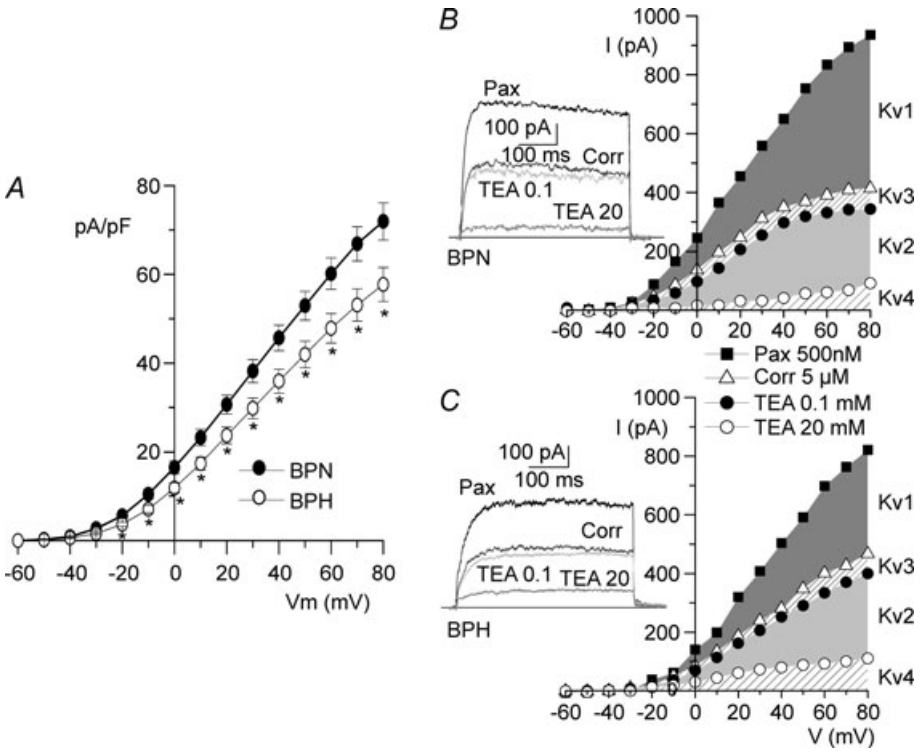

Figure 4. Pharmacological characterization of Kv currents
A, total Kv current density *versus* voltage curves were obtained after blockade of BK_{Ca} current with 500 nM paxilline in BPN (●) and BPH (○) VSMCs; $n = 22$ cells in each group, $^*P < 0.05$. Representative examples of the protocol for pharmacological dissection of the Kv currents are shown for one BPN (*B*) and one BPH (*C*) cell. The graphs show the *I–V* relationships in the presence of 500 nM paxilline (total Kv current), after application of 5 μM correolide, and in the presence of two TEA concentrations. The contribution of each component (Kv1–Kv4) is represented by the shaded areas. Traces show the currents obtained upon depolarization to +40 mV with each of the blockers.

Figure 4*B* and *C* show that in both BPN and BPH VSMCs, Kv1 (the correolide-sensitive current) and Kv2 (the current sensitive to 20 mM TEA) represented together 86% of the total Kv currents of the BPN cell and 83% of the BPH cell. There was a minimal contribution of Kv3 currents (the current blocked by 100 μM TEA) and Kv4 currents (the residual current after 20 mM TEA). This latter component is most likely over-estimated, as rapidly inactivating 'A-type' currents were not recorded in these cells.

The use of selective Kv2 blockers, such as stromatoxin (ScTx) or guangxitoxin (GxTx) (Amberg & Santana, 2006; Herrington *et al.* 2006), allowed us to explore in more detail the relative contribution of Kv1 and Kv2 channels in both preparations. Figure 5 shows averaged conductance–voltage curves obtained in both groups (BPN and BPH) in the presence of paxilline (control) and after application of either Kv1 or Kv2 blockers. Kv1 conductance averaged 0.17 ± 0.01 nS pF^{-1} in BPN and 0.10 ± 0.02 nS pF^{-1} in BPH. Although the decrease in Kv1 conductance in BPH cells was significant, their percentual contribution to the total Kv conductance was the same in BPN and BPH cells, since there were no significant differences in correolide effect when expressed as percentage inhibition (Fig. 5*C*). In contrast, both the conductance and the percentual contribution of Kv2 currents (defined as the ScTx sensitive currents) were significantly smaller in BPH cells (Fig. 5*B* and *D*). The same results were obtained when comparing the 20 mM TEA-induced inhibition (after correolide application). However, whilst the effect of 20 nM GxTx was similar to that of 50 nM ScTX in BPN currents, it was significantly smaller on BPH currents, suggesting a lower affinity of GxTx for Kv2 channels in BPH cells.

Functional characterization of Kv2 currents in VSMCs

In addition to the decreased amplitude of the Kv2 component in BPH cells, we consistently observed a slower activation and deactivation of BPH currents (see

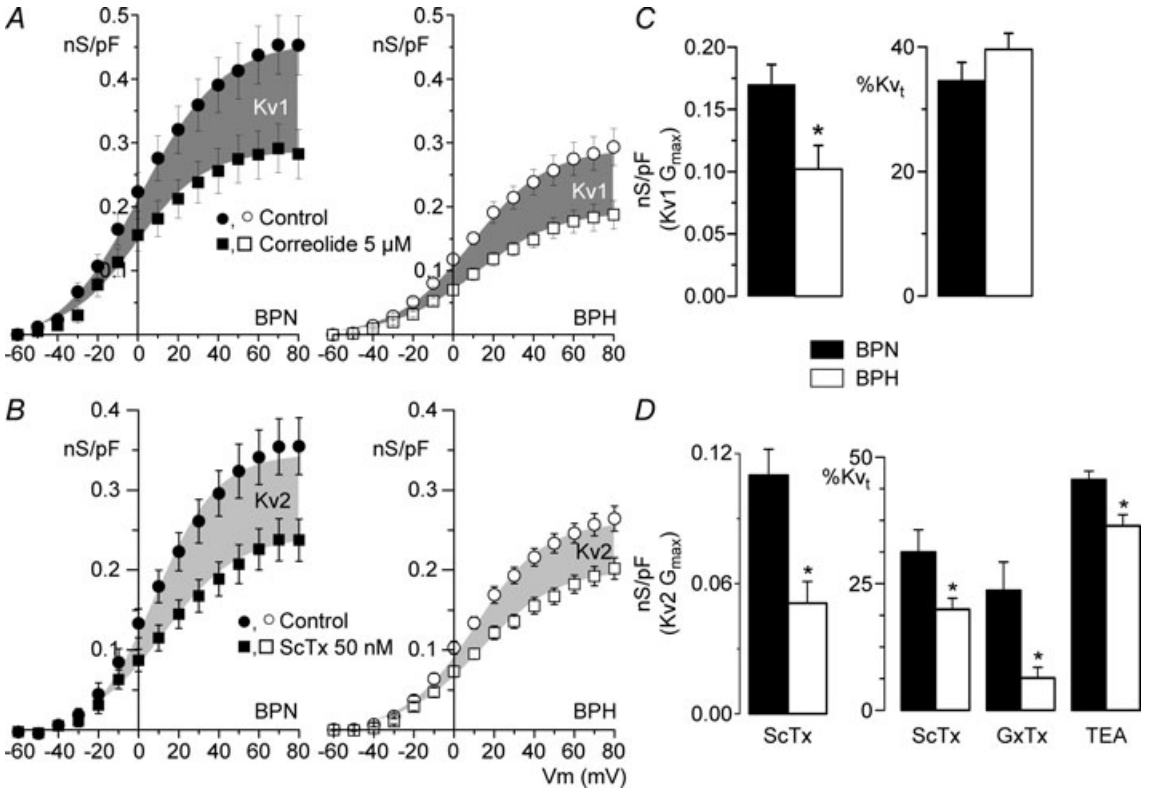

Figure 5. Quantification of Kv1 and Kv2 contribution to Kv currents
Conductance (nS pF^{-1})–voltage relationships obtained in BPN (●, ■) and BPH (○, □) cells in the presence of 500 nM paxilline (control) and after application of 5 μM correolide (*A*) or 50 nM ScTx (*B*). Data points are means ± S.E.M.; $n = 8$–12 in each group. The shaded areas are delimited by the Boltzmann fits of the two curves and represent the correolide-sensitive (Kv1) and ScTx-sensititive (Kv2) fractions of the total conductance. G_{max} values for the Kv1 (*C*) and Kv2 (*D*) components were obtained by subtracting the G_{max} of the drug-resistant from the G_{max} of the control *G–V* fits to Boltzmann functions in each cell. Right graph bars show the percentual contribution of Kv1 (*C*) and Kv2 (*D*) computed as percentage of total Kv conductance (Kv_t) at +40 mV. The proportion of the Kv2 component was also studied by using 20 nM GxTx and 20 mM TEA (after correolide). Means ± S.E.M. of 7–12 data.

Figs 2 and 4) that could be attributable to the kinetic behaviour of the Kv2 channels. To explore these parameters in more detail, we performed a set of experiments to study the correolide-resistant fraction of the currents (mainly carried by Kv2 channels) in symmetrical K^+ concentrations. Representative traces in both preparations are shown in Fig. 6*A*. Under these conditions, the activation time was analysed by measuring the rising time (arbitrarily defined as the time to reach 75% of the peak current amplitude from the onset of a depolarizing pulse to +40 mV). Our data show a significant increase of this parameter in BPH currents. The deactivation time course was studied by fitting the tail currents elicited upon repolarization to a biexponential function. The clear slow-down observed in BPH currents could be explained by an increase in the amplitude of the slow component of the fit together with an increase in the slow time constant (Fig. 6*B*). Finally, a significant shift of the voltage dependence of the activation towards more hyperpolarized potentials in BPH currents was also obtained by the analysis of the conductance curves in both preparations (Fig. 6*C*).

We hypothesized that these differences could be a consequence of the *de novo* expression of Kv6.3 subunits in BPH cells. In fact, immunoblots with anti-Kv6.3 antibody in protein extracts from mesenteric arteries show expression of this protein in BPH but not in BPN arteries (Fig. 7*A*). These differences were not observed when comparing protein extracts from BPN and BPH aortas (data not shown). In order to obtain more direct evidence of a possible functional role of Kv6.3 channels in BPH animals, the effect of intracellular application of anti-Kv6.3 antibody on Kv currents was studied with the voltage-clamp protocol described in Methods (Archer *et al.* 1998; Sanchez *et al.* 2002). Once the whole-cell configuration was achieved, the baseline

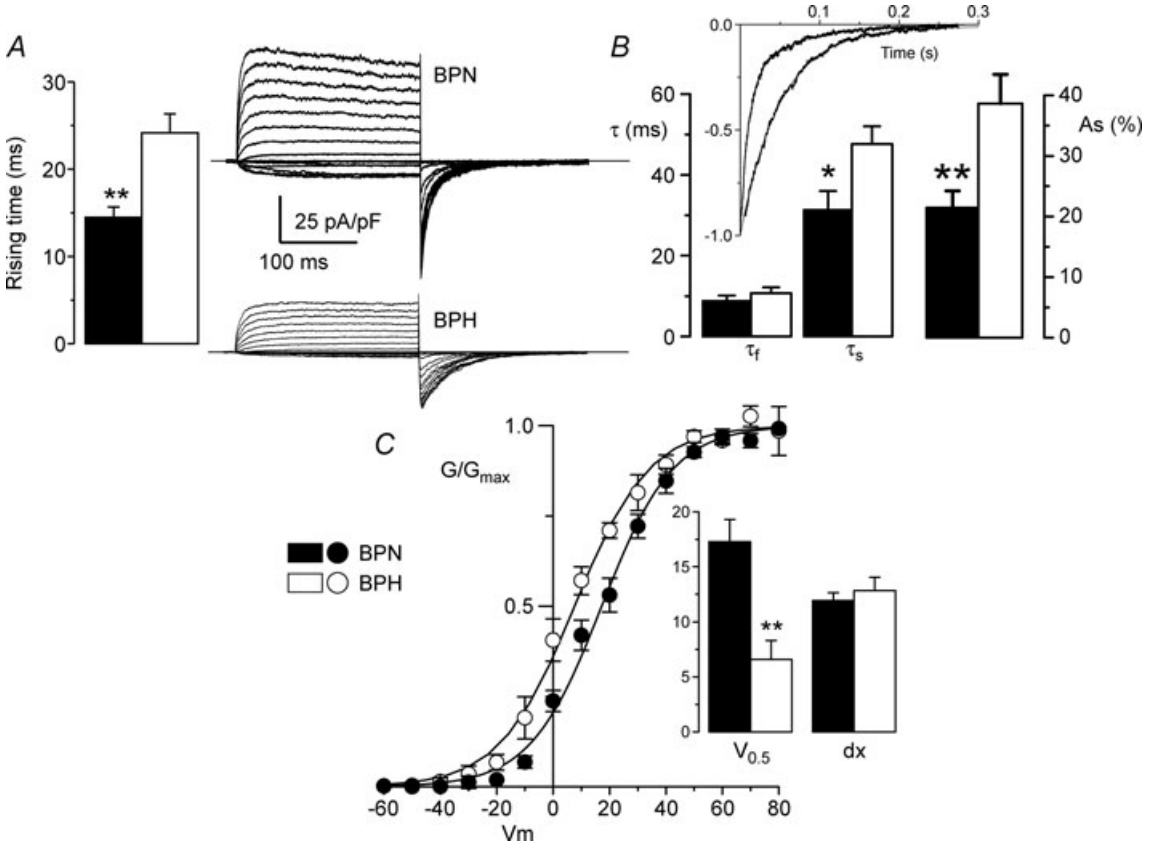

Figure 6. Kinetic characterization of Kv2 currents in mesenteric VSMCs
Activation and deactivation parameters (*A* and *B*) were studied in symmetrical K^+ solutions and in the presence of 500 nM paxilline and 5 μM correolide. Representative traces of a family of currents from BPN and BPH cells are shown (*A*). Time course of activation was studied by measuring the rising time in depolarizing pulses from −80 to +40 mV. *B*, time course of deactivation was obtained from the fit of the tail currents to a biexponential function. The inset shows the normalized tail currents from the examples shown in *A* and their corresponding fits; $n = 8$. *C*, normalized conductance curves were obtained from the ScTx-sensitive component of BPN and BPH currents. The continuous lines are the Boltzmann fit of the data. The inset shows the mean of the slopes (d*x*) and the voltages ($V_{0.5}$) for half-activation obtained from the Boltzmann fits of each individual cell; $n = 7$.

currents were allowed to stabilized (usually after 4–5 min), as a run-up of the current was generally observed during the first minutes of recording. Within 15 min of recording, dialysis of the anti-Kv6.3 antibody did not change the current amplitude in BPN cells (upper traces), while in all BPH cells tested there was an irreversible decrease of the initial current amplitude (lower traces). Recordings in the presence of antibodies for as long as 35 min did not increase significantly the observed inhibition. The average effects of the antibodies applied in this study are shown in Fig. 7*B*. Anti-Kv6.3 produced a significant reduction of the Kv currents only in BPH cells (14.03 ± 1.5) while no changes were observed in BPN cells (-0.28 ± 0.6). As an additional control, Kv currents were recorded in BPH cells with anti-Kv3.1 antibody in the pipette, as Kv3.1 mRNA was not detected in our initial screening (see above). Under this condition, no significant changes were observed in the current amplitude after 15–20 min of recording (the average percentage inhibition on 6 cells was -0.35 ± 0.5).

To further support our hypothesis, we explored the modulatory effects of Kv6.3 coexpression on Kv2.1 currents using the heterologous expression of these two channel proteins in HEK293 cells. Coexpression of Kv6.3 leads to kinetic and pharmacological modifications of Kv2.1 currents that adequately reproduce the modifications observed in the BPH VSMCs. We observed a significant decrease of the current amplitude of the heteromultimeric Kv6.3/Kv2.1 channels, a slowdown of the activation and deactivation time course and a leftward shift of the half-maximal value of the steady state activation curve (Fig. 8). Moreover, when we explored the sensitivity of Kv2.1 or Kv2.1/Kv6.3 channels to the different Kv2 blockers, we found that in the presence of Kv6.3 there was a reduced sensitivity to GxTx, while the effect of ScTx and TEA were comparable in the two groups.

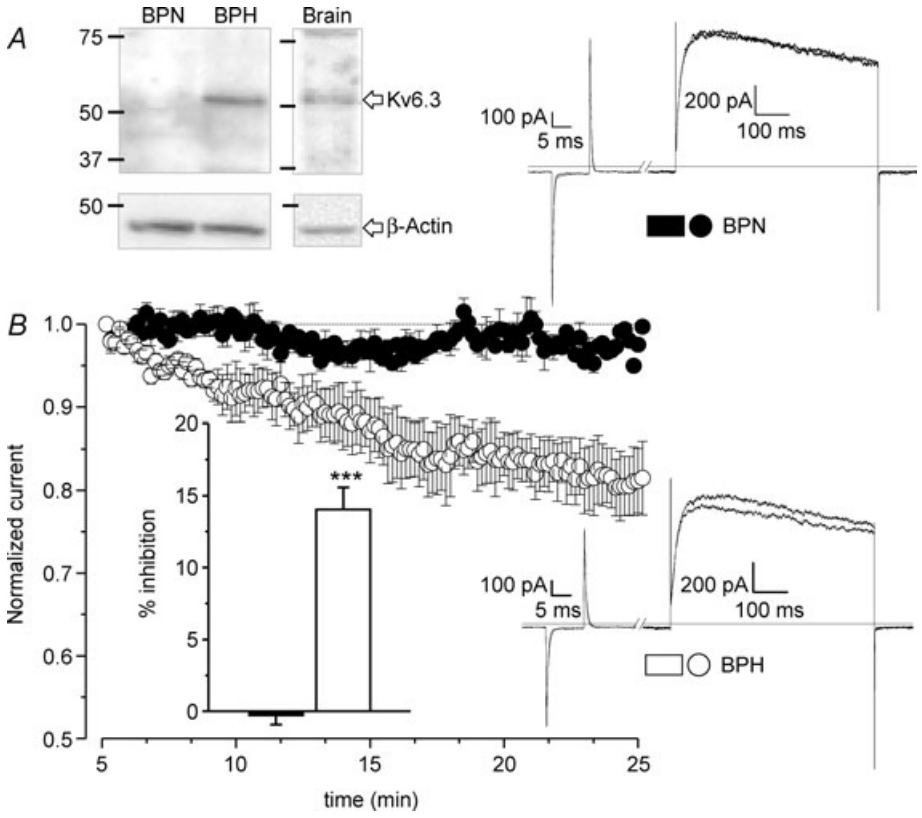

Figure 7. Characterization of the expression of Kv6.3 protein in BPN and BPH mesenteric VSMCs
A, the presence of Kv6.3 subunits in BPN and BPH mesenteric arteries was analysed by Western blot. Mouse brain was the positive control and immunoblot with β-actin providing the loading control. The figure is representative of 4 different experiments. *B*, the functional contribution of Kv6.3 subunits to Kv currents was explored by analysing the effect of the intracellular application of anti-Kv6.3 antibodies on the current amplitude. The graph shows the normalized time course of the current amplitude in BPN and BPH cells up to 25 min after the establishment of the whole-cell configuration. Data are means ± S.E.M. of 5–7 cells. The inset represents the average inhibition obtained at 20 min in BPN (black bar) and BPH cells (white bar). Representative traces from one BPN and one BPH cell at two different time points (5 and 20 min) are also shown. These records were obtained with the protocol described in the methods section.

Role of Kv currents in VSMCs excitability

In order to determine the relative contribution of Kv channels to resting E_M and hence their contribution to cell excitability, current-clamp experiments have been carried out in freshly dissociated cells from both BPN and BPH mesenteric arteries (Fig. 9). We found that E_M values at rest were more depolarized in BPH as compared to BPN (-43.63 ± 0.97 *versus* -51.00 ± 1.43 mV). We have also studied the changes in this resting E_M induced by the blockade of BK channels (by using 500 μM paxilline), Kv1 channels (by applying 5 μM correolide) and Kv2 channels (by using either 50 nM ScTX or 20 nM GxTx). While paxilline had no effect on E_M, all the other drugs tested were able to elicit depolarizations in both preparations. No differences in the magnitude of these effects were observed when comparing BPN and BPH cells, with the exception of a significant decrease in the depolarization elicited by GxTx in BPH cells.

Discussion

We have explored the changes in expression of a large number of K^+ channel genes (Kv channels, BK channels and their accessory subunits) in two different vascular beds (mesenteric and aortic vessels) and two different mice strains (BPN and BPH). The characterization of the mRNA changes in expression has been used to look for correlations at the functional level, by exploring the contribution of the different channel subfamilies to the total outward current and to set the resting E_M of freshly dispersed VSMCs. Our findings show that both the expression pattern of these channels genes and the hypertension-induced changes are vascular bed specific. To our knowledge, this is the first comprehensive characterization of the expression pattern in a murine model of hypertension.

In the hypertensive (BPH) mesenteric VSMCs, the most conspicuous finding in terms of mRNA expression, the

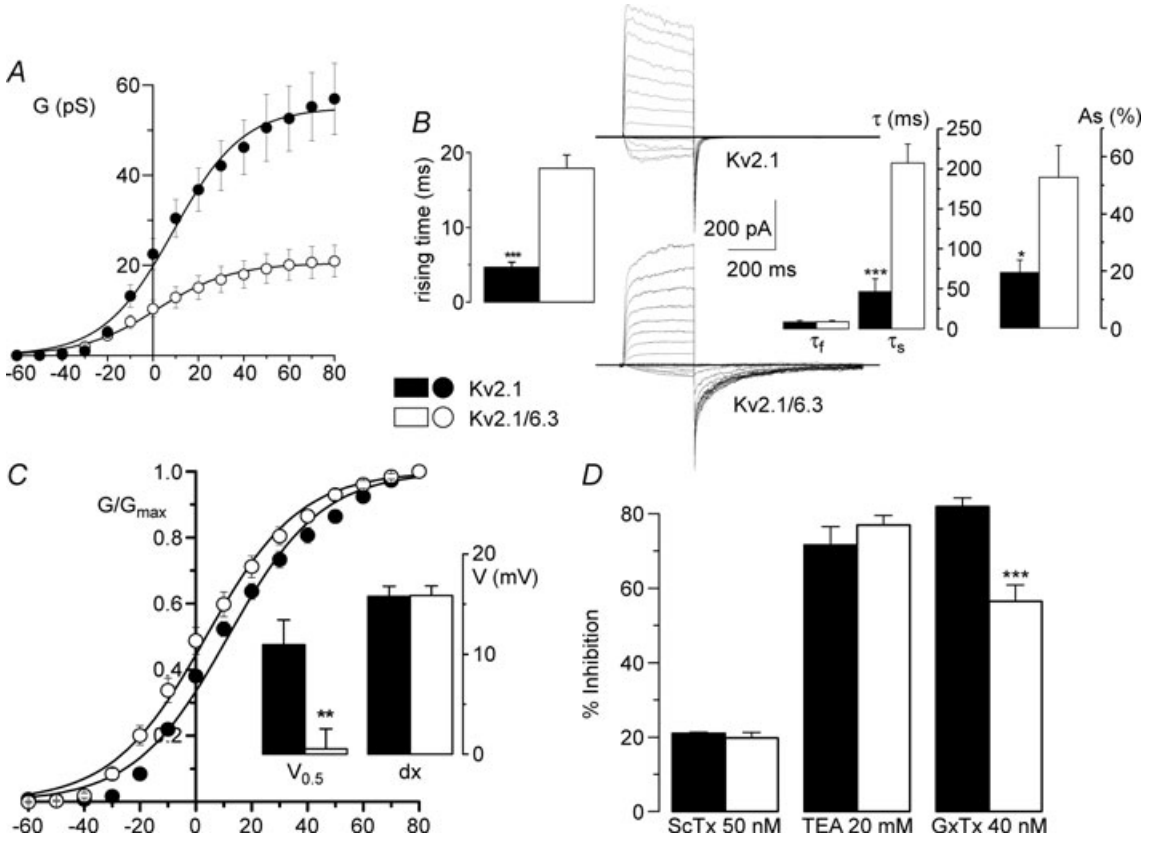

Figure 8. Characterization of Kv2.1 and Kv2.1/Kv6.3 currents in HEK cells
A, conductance curves obtained from HEK cells transfected with Kv2.1 alone (●) or Kv2.1 + Kv6.3 (○). Lines show the fit of the data to Boltzmann functions; $n = 10$–11 cells. *B*, symmetrical K^+ solutions were used to study the kinetics of the current. The figure shows representative traces obtained in depolarizing pulses from −60 to +80 mV and the analysis of activation (rising time) and deactivation (tail currents) performed in 10 cells in each group. *C*, normalized conductance curves from Kv2.1 and Kv2.1/Kv6.3 currents were obtained and analysed as in Figure 6. *D*, the effect of different blockers of Kv2 currents is expressed as percentage of inhibition of the current elicited at +40 mV. Means ± S.E.M. of 5–7 cells.

de novo expression of Kv6.3, shows a very good correlation with the levels of protein expression (determined by Western blot) and with the electrophysiological properties of the freshly isolated cells. We found a significant decrease in the Kv current density of mesenteric BPH VSMCs, which can be attributed to the decreased amplitude of the Kv1 and Kv2 components of the current. However, although percentual contribution of Kv1 to total Kv is identical in BPN and BPH VSMCs, the contribution of Kv2 was significantly smaller in BPH cells. The decreased expression of KChAP, a well known chaperon for Kv1 subunits, could explain the reduced Kv1 conductance in BPH (Kuryshev *et al.* 2000). Changes in the kinetics and in the pharmacological profile of BPH currents can be reproduced in an heterologous expression system by coexpression of Kv6.3 with Kv2.1 channels. The Kv6.3 subunit belongs to one of the subfamilies of electrically silent Kv α subunits (γ subunits), which comprises all the members of the Kv5–Kv6 and Kv8–Kv9 families. These subunits do not form functional channels when expressed on their own, but coassemble with Kv2.1 and Kv2.2 subunits to produce heterotetrameric channels (Post *et al.* 1996; Salinas *et al.* 1997; Kramer *et al.* 1998; Ottschytsch *et al.* 2002). Reported differences in Kv2 channels upon γ subunit coexpression include decrease in the current amplitude, changes in the voltage dependence of activation and inactivation, in the time course of activation, inactivation and deactivation and in the drug sensitivity of the heteromultimeric channels. In the case of Kv6.3, there are only a few studies (Ottschytsch *et al.* 2002; Sano *et al.* 2002; Vega-Saenz de Miera, 2004) in which the modifications reported are not fully coincident, and for this reason we have carried out the comparative study (Kv2.1 *versus* Kv2.1/Kv6.3 currents) in transfected HEK cells. We found a decrease of the current amplitude in heteromeric Kv2.1/Kv6.3 that has been previously reported in one of the above-mentioned studies (Vega-Saenz de Miera, 2004) but was not explored in the others. Regarding the kinetic changes, we saw a significant slowdown of activation (in agreement with the data of Vega-Saenz de Miera but opposite to the report of Ottschytsch *et al.*) and deactivation (reported by Sano *et al.* 2002), but found to be not significant in the work of Ottschytsch *et al.* Finally, we saw a leftward shift in the steady-state activation curve in the presence of Kv6.3 channels as reported by Ottschytsch *et al.* but not by Sano *et al.* It is likely that the differences in the expression systems used (oocytes, L929 and Ltk cells) as well as in the ratio of Kv2.1 : Kv6.3 (Vega-Saenz de Miera, 2004) contribute to the observed discrepancies.

Our data indicate that all the differences in the native Kv2 currents between BPN and BPH preparations can be readily explained assuming that while in BPN VSMCs these currents are carried by homomultimeric Kv2.1, in BPH cells they are mainly mediated by Kv2.1/Kv6.3 heterocomplexes. The slight differences in the kinetics of the currents when comparing Kv2.1/Kv6.3 complexes in HEK cells and BPH Kv2 currents are most likely due to the increased Kv6.3 : Kv2.1 ratio in HEK cells (designed to augment the probability of heteromultimeric channels), so that the effects of Kv6.3 expression are exaggerated. Our conclusion is also fully supported by the mRNA and protein expression data, and by the functional blockade

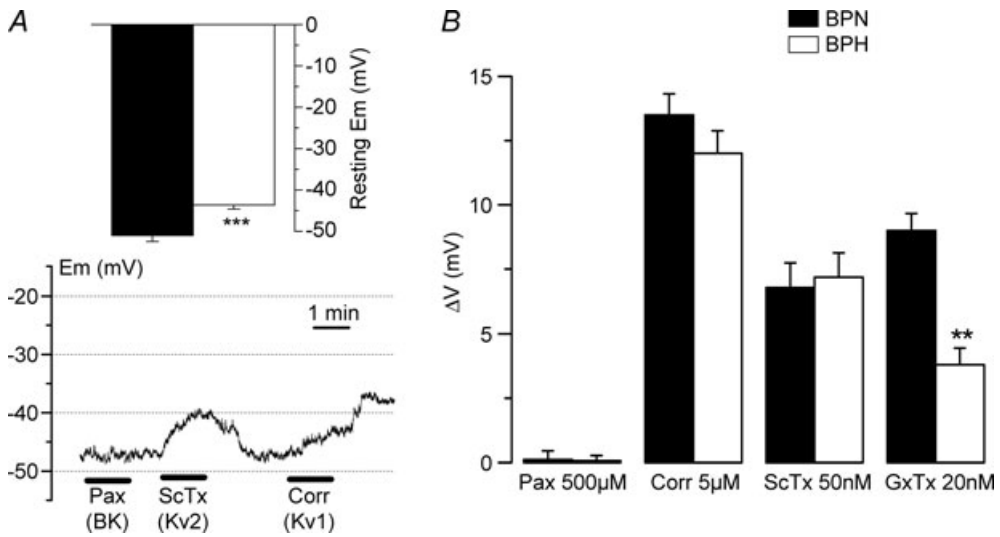

Figure 9. Resting E_M in BPN and BPH VSMCs
A, values of resting E_M obtained in current-clamp experiments with the perforated-patch configuration from BPH and BPN mesenteric VSMCs; $n = 39$. The lower graph shows resting E_M values in one BPN cell during the application of 500 nM paxilline, 50 nM ScTx and 5 μM correolide as indicated with the bars. *B*, the average depolarization (means ± S.E.M.) obtained in 9–15 BPN and BPH cells with the different drugs explored is represented as ΔV_m.

of the currents with anti-Kv6.3 antibody. The immunological blockade of Kv channels is a powerful tool to assay the role of a particular channel subunit under the different physiological conditions that have been widely used (Archer *et al.* 1998; Conforti *et al.* 2000; Sanchez *et al.* 2002; Archer *et al.* 2004). Although the lack of an estimation of the affinity of the antibody prevented us from extracting conclusive results about the quantitative contribution of Kv6.3-containing channels to Kv2 currents in BPH cells, the fact that we saw a decrease of the current in all BPH cells studied and in none of the BPN cells tested allows us to conclude that Kv6.3 protein is not functionally expressed in BPN cells, and that functional Kv2.1/Kv6.3 heteromultimers are present in BPH cells. Additionally, even the pharmacological profile of Kv currents is consistent with this interpretation, and lets us propose that GxTx could be a useful tool to investigate the molecular correlate of Kv2 currents, as its potency greatly decreases in the presence of the accessory subunit Kv6.3.

The molecular coding of Kv channels is central to the proper function of different types of smooth muscle cells. In VSMCs, several lines of evidence indicate that Kv1 channels have a dominant role in opposing excitability, and by regulating E_M at physiological relevant potentials represent a critical negative feedback mechanism to determine the extent of myogenic constriction (Albarwani *et al.* 2003; Fountain *et al.* 2004; Plane *et al.* 2005; Chen *et al.* 2006). This body of work has provided strong support to the idea that Kv1 dysfunction may contribute to vascular pathologies such as vasospasm and hypertension. However, differences in the functional contribution of other K^+ channels (particularly Kv2 and BK_{Ca}, and also other inward currents) acts in concert with Kv1 channels to determine VSMC E_M (Brayden & Nelson, 1992; Ledoux *et al.* 2006; Amberg & Santana, 2006). Interestingly, the changes in K^+ channels expression profile in genetic or induced models of hypertension consistently points towards the involvement of changes in non-Kv1 channels at the pathogenesis of the altered vascular tone. Angiotensin-II induced hypertension in rats is associated with down-regulation of the β1 subunit of BK_{Ca} in cerebral VSMCs (Amberg *et al.* 2003). The same changes have been found in genetic hypertension (Amberg & Santana, 2003) and are consistent with results obtained in β1-knockout mice (Brenner *et al.* 2000). In this regard, we show here that there is a down-regulation of the expression levels of BK_{Ca} α and β1 mRNA in BPH VSMCs (Fig. 1) and our functional study points to a decreased amplitude of BK_{Ca} currents and more importantly, a decreased sensitivity of the currents to Ca^{2+} modulation in this preparation (Fig. 3). Although more in-depth studies should be carried out to confirm the physiological role of BK_{Ca} channels in our model and their contribution to the development of hypertension, the preliminary data presented here are in agreement with previous data in the literature (Brenner *et al.* 2000; Amberg *et al.* 2003; Sausbier *et al.* 2005).

Impaired Kv2 channel activity has also been shown to contribute to arterial dysfunction during angiotensin-II-dependent hypertension (Amberg & Santana, 2006). However, there are considerable discrepancies in the literature regarding the contribution of different ion channels to the altered vascular tone during hypertension, due to differences in the experimental design, in the hypertensive model studied and, probably most importantly, in the types of vascular preparations used. As hypertension-induced changes in the expression profile of the channels are vascular-bed specific, the characterization of this expression profile is a prerequisite to determine the functional impact of the hypertension-induced changes in a given preparation.

Our findings provide molecular and functional evidence to support the hypothesis that *de novo* expression of the accessory subunit Kv6.3 (which leads to modulation of Kv2 currents) may be an active component in the natural development of hypertension. Up-regulation of the *Kcng3* gene was found in mesenteric and not in aortic VSMCs, Kv6.3 protein was detected in BPH (and not in BPN) mesenteric VSMCs, the functional characterization of Kv currents in mesenteric cells shows changes consistent with the presence of heterotetrameric Kv2.1/Kv6.3 channels and the blockade experiments with anti-Kv6.3 antibody demonstrates a functional role of this subunit only in hypertensive VSMCs. VSMCs from hypertensive vessels are more depolarized and show a significantly decrease of K^+ currents, findings that are consistent with their hypertensive state. This more depolarized resting E_M would result in higher resting tone of the vessels, contributing to the increased vascular resistance in hypertension. When exploring the contribution of the currents to resting E_M we observe that in our experimental conditions (very low $[Ca^{2+}]$), both Kv1 and Kv2 currents, but not BK_{Ca} currents, contribute to determine resting E_M. Surprisingly, we found no differences in the contribution of Kv1 and Kv2 channels to set resting E_M between BPN and BPH cells. Although the overall current amplitude of the Kv2 component is decreased in BPH cells, the shift in the voltage dependence of activation towards more hyperpolarized potentials makes plausible that their contribution at values near the resting E_M of the cells is unchanged. This observation implies that in addition to the decrease in both BK_{Ca} and Kv currents, there must be changes in other non-Kv conductances in the BPH mesenteric VSMCs that would be responsible for the more depolarized resting E_M. Nevertheless, the observed changes in the contribution of Kv1 and Kv2 channels to the total Kv conductance, together with the kinetic changes in Kv2 currents mediated by Kv2/Kv6.3 heteromultimers would be expected to cause significant changes in the pressure-induced contractile response of

myogenically active vessels. These findings could provide new insights to understand the molecular basis for the vascular dysfunction during hypertension.

References

Albarwani S, Nemetz LT, Madden JA, Tobin AA, England SK, Pratt PF & Rusch NJ (2003). Voltage-gated K^+ channels in rat small cerebral arteries: molecular identity of the functional channels. *J Physiol* **551**, 751–763.

Amberg GC, Bonev AD, Rossow CF, Nelson MT & Santana LF (2003). Modulation of the molecular composition of large conductance, Ca^{2+} activated K^+ channels in vascular smooth muscle during hypertension. *J Clin Invest* **112**, 717–724.

Amberg GC & Santana LF (2003). Downregulation of the BK channel β1 subunit in genetic hypertension. *Circ Res* **93**, 965–971.

Amberg GC & Santana LF (2006). Kv2 channels oppose myogenic constriction of rat cerebral arteries. *Am J Physiol Cell Physiol* **291**, C348–C356.

Archer SL, Souil E, Dinh-Xuan AT, Schremmer B, Mercier JC, El Yaagoubi A, Nguyen-Huu L, Reeve HL & Hampl V (1998). Molecular identification of the role of voltage-gated K^+ channels, Kv1.5 and Kv2.1, in hypoxic pulmonary vasoconstriction and control of resting membrane potential in rat pulmonary artery myocytes. *J Clin Invest* **101**, 2319–2330.

Archer SL, Wu XC, Thebaud B, Nsair A, Bonnet S, Tyrrell B, McMurtry MS, Hashimoto K, Harry G & Michelakis ED (2004). Preferential expression and function of voltage-gated, O_2-sensitive K^+ channels in resistance pulmonary arteries explains regional heterogeneity in hypoxic pulmonary vasoconstriction: ionic diversity in smooth muscle cells. *Circ Res* **95**, 308–318.

Brayden JE & Nelson MT (1992). Regulation of arterial tone by activation of calcium-dependent potassium channels. *Science* **256**, 532–535.

Brenner R, Perez GJ, Bonev AD, Eckman DM, Kosek JC, Wiler SW, Patterson AJ, Nelson MT & Aldrich RW (2000). Vasoregulation by the β1 subunit of the calcium-activated potassium channel. *Nature* **407**, 870–876.

Chen TT, Luykenaar KD, Walsh EJ, Walsh MP & Cole WC (2006). Key role of Kv1 channels in vasoregulation. *Circ Res* **99**, 53–60.

Cheong A, Dedman AM & Beech DJ (2001*a*). Expression and function of native potassium channel Kvα1 subunits in terminal arterioles of rabbit. *J Physiol* **534**, 691–700.

Cheong A, Dedman AM, Xu SZ & Beech DJ (2001*b*). Kvα1 channels in murine arterioles: differential cellular expression and regulation of diameter. *Am J Physiol Heart Circ Physiol* **281**, H1057–H1065.

Coetzee WA, Amarillo Y, Chiu J, Chow A, Lau D, McCormack T, Moreno H, Nadal MS, Ozaita A, Pountney D, Saganich M, Vega-Saenz de Miera E & Rudy B (1999). Molecular diversity of K^+ channels. *Ann N Y Acad Sci* **868**, 233–285.

Cole WC, Chen TT & Clement-Chomienne O (2005). Myogenic regulation of arterial diameter: role of potassium channels with a focus on delayed rectifier potassium current. *Can J Physiol Pharmacol* **83**, 755–765.

Conforti L, Bodi I, Nisbet JW & Millhorn DE (2000). O_2-sensitive K^+ channels: role of the Kv1.2-subunit in mediating the hypoxic response. *J Physiol* **524**, 783–793.

Cox RH (2002). Changes in the expression and function of arterial potassium channels during hypertension. *Vascular Pharmacol* **38**, 13–23.

Cox RH & Rusch NJ (2002). New expression profiles of voltage-gated ion channels in arteries exposed to high blood pressure. *Microcirculation* **9**, 243–257.

Fountain SJ, Cheong A, Flemming R, Mair L, Sivaprasadarao A & Beech DJ (2004). Functional up-regulation of KCNA gene family expression in murine mesenteric resistance artery smooth muscle. *J Physiol* **556**, 29–42.

Friese RS, Mahboubi P, Mahapatra NR, Mahata SK, Schork NJ, Schmid-Schonbein GW & O'Connor DT (2005). Common genetic mechanisms of blood pressure elevation in two independent rodent models of human essential hypertension. *Am J Hypertens* **18**, 633–652.

Hanner M, Schmalhofer WA, Green B, Bordallo C, Liu J, Slaughter RS, Kaczorowski GJ & Garcia ML (1999). Binding of correolide to Kv1 family potassium channels: Mapping the domains of high affinity interaction. *J Biol Chem* **274**, 25237–25244.

Herrington J, Zhou YP, Bugianesi RM, Dulski PM, Feng Y, Warren VA, Smith MM, Kohler MG, Garsky VM, Sanchez M, Wagner M, Raphaelli K, Banerjee P, Ahaghotu C, Wunderler D, Priest BT, Mehl JT, Garcia ML, McManus OB, Kaczorowski GJ & Slaughter RS (2006). Blockers of the delayed-rectifier potassium current in pancreatic β-cells enhance glucose-dependent insulin secretion. *Diabetes* **55**, 1034–1042.

Jackson WF (2000). Ion channels and vascular tone. *Hypertension* **35**, 173.

Jackson WF (2005). Potassium channels in the peripheral microcirculation. *Microcirculation* **12**, 113–127.

Kohler R, Wulff H, Eichler I, Kneifel M, Neumann D, Knorr A, Grgic I, Kampfe D, Si H, Wibawa J, Real R, Borner K, Brakemeier S, Orzechowski HD, Reusch HP, Paul M, Chandy KG & Hoyer J (2003). Blockade of the intermediate-conductance calcium-activated potassium channel as a new therapeutic strategy for restenosis. *Circulation* **108**, 1119–1125.

Kramer JW, Post MA, Brown AM & Kirsch GE (1998). Modulation of potassium channel gating by coexpression of Kv2.1 with regulatory Kv5.1 or Kv6.1 α-subunits. *Am J Physiol Cell Physiol* **274**, C1501–C1510.

Kuryshev YA, Gudz TI, Brown AM & Wible BA (2000). KChAP as a chaperone for specific K^+ channels. *Am J Physiol Cell Physiol* **278**, C931–C941.

Ledoux J, Werner ME, Brayden JE & Nelson MT (2006). Calcium-activated potassium channels and the regulation of vascular tone. *Physiology* **21**, 69–78.

Li G & Cheung DW (1999). Effects of paxilline on K^+ channels in rat mesenteric arterial cells. *Eur J Pharmacol* **372**, 103–107.

Livak KJ & Schmittgen TD (2001). Analysis of relative gene expression data using real-time quantitative PCR and the $2^{-\Delta\Delta Ct}$ method. *Methods* **25**, 402–408.

Mackie AR, Brueggemann LI, Henderson KK, Shiels AJ, Cribbs LL, Scrogin KE & Byron KL (2008). Vascular KCNQ potassium channels as novel targets for the control of mesenteric artery constriction by vasopressin, based on studies in single cells, pressurized arteries, and in vivo measurements of mesenteric vascular resistance. *J Pharmacol Exp Ther* **325**, 475–483.

Miguel-Velado E, Moreno-Dominguez A, Colinas O, Cidad P, Heras M, Perez-Garcia MT & López-López JR (2005). Contribution of Kv channels to phenotypic remodeling of human uterine artery smooth muscle cells. *Circ Res* **97**, 1280–1287.

Mulvany MJ (2002). Small artery remodeling and significance in the development of hypertension. *News Physiol Sci* **17**, 105–109.

Nelson MT & Quayle JM (1995). Physiological roles and properties of potassium channels in arterial smooth muscle. *Am J Physiol Cell Physiol* **268**, C799–C822.

Ottschytsch N, Raes A, Van Hoorick D & Snyders DJ (2002). Obligatory heterotetramerization of three previously uncharacterized Kv channel α-subunits identified in the human genome. *Proc Natl Acad Sci U S A* **99**, 7986–7991.

Plane F, Johnson R, Kerr P, Wiehler W, Thorneloe K, Ishii K, Chen T & Cole W (2005). Heteromultimeric Kv1 channels contribute to myogenic control of arterial diameter. *Circ Res* **96**, 216–224.

Post MA, Kirsch GE & Brown AM (1996). Kv2.1 and electrically silent Kv6.1 potassium channel subunits combine and express a novel current. *FEBS Lett* **399**, 177–182.

Salinas M, Duprat F, Heurteaux C, Hugnot JP & Lazdunski M (1997). New modulatory α subunits for mammalian Shab K^+ channels. *J Biol Chem* **272**, 24371–24379.

Sanchez D, López-López JR, Perez-Garcia MT, Sanz-Alfayate G, Obeso A, Ganfornina MD & Gonzalez C (2002). Molecular identification of Kvα subunits that contribute to the oxygen-sensitive K^+ current of chemoreceptor cells of the rabbit carotid body. *J Physiol* **542**, 369–382.

Sano Y, Mochizuki S, Miyake A, Kitada C, Inamura K, Yokoi H, Nozawa K, Matsushime H & Furuichi K (2002). Molecular cloning and characterization of Kv6.3, a novel modulatory subunit for voltage-gated K^+ channel Kv2.1. *FEBS Lett* **512**, 230–234.

Sausbier M, Arntz C, Bucurenciu I, Zhao H, Zhou XB, Sausbier U, Feil S, Kamm S, Essin K, Sailer CA, Abdullah U, Krippeit-Drews P, Feil R, Hofmann F, Knaus HG, Kenyon C, Shipston MJ, Storm JF, Neuhuber W, Korth M, Schubert R, Gollasch M & Ruth P (2005). Elevated blood pressure linked to primary hyperaldosteronism and impaired vasodilation in BK channel-deficient mice. *Circulation* **112**, 60–68.

Schlager G & Sides J (1997). Characterization of hypertensive and hypotensive inbred strains of mice. *Laboratory Anim Sci* **47**, 288–292.

Vega-Saenz de Miera EC (2004). Modification of Kv2.1 K^+ currents by the silent Kv10 subunits. *Brain Res Mol Brain Res* **123**, 91–103.

Yeung SYM, Pucovsky V, Moffatt JD, Saldanha L, Schwake M, Ohya S & Greenwood IA (2007). Molecular expression and pharmacological identification of a role for Kv7 channels in murine vascular reactivity. *Br J Pharmacol* **151**, 758–770.

Acknowledgements

We thank Esperanza Alonso for excellent technical assistance, Merck Company for correolide and GxTx, and D. J. Snyder for Kv2.1 and Kv6.3 plasmids. This work was supported by Ministerio de Sanidad y Consumo, Instituto de Salud Carlos III grants R006/009 (Red Heracles) and PI041044 (J.R.L.L.) and Ministerio de Educación y Ciencia grants BFU2004–05551 (M.T.P.G.) and BFU2007-61524 (J.R.L.L.).